ARTICLE   OPEN

Check for updates

A new Asian/North American teleconnection linking clustered extreme precipitation from Indian to Canada

Bin Wang [iD][1,2], Ming-Ying Lee[3], Zhiling Xie [iD][1,2], Mengqian Lu [iD][4 ✉] and Mengxin Pan [iD][4]

Three consecutive precipitation extremes emerged in November 2021, including India-Sri Lanka flooding, East Asian blizzard, and Canadian floods. Why the catastrophic events occurred successively and whether they will become more frequent as global warming continues are unknown. Here we show they are organized by an intraseasonal Asian/North American (ANA) teleconnection consisting of two cross-Pacific wave trains fortified by dipolar diabatic heating anomalies ("wet India-dry Philippines"). The dipolar heating anomaly is shaped by multi-scale interaction between a quasi-stationary Madden-Julian Oscillation (MJO) episode and a rapidly developed La Niña over the tropical Asian monsoon region. Numerical experiments suggest that the off-equatorial heating dipole can generate the ANA pattern resembling observations, distinct from the equatorial MJO-induced teleconnection and the La Niña-induced Pacific/North American teleconnection. Philippine cooling stimulates the circum-Pacific wave train, while Indian heating produces the eastward-propagating subtropical wave train. These wave trains persistently steered cross-Pacific atmospheric rivers channeling warm-moisture-laden air to the extratropics. We suggest that the ANA teleconnection could be a new route by which multi-scale interaction between the La Niña and quasi-stationary MJO over the tropical Asian monsoon affects extratropical East Asia and North America. This work provides a unique perspective on understanding the origins of increasing collisions of extremes worldwide within a short time as the global climate warms.

INTRODUCTION

On November 3–8th, 2021, India and Sri Lanka were hit by heavy rain and severe flooding (Fig. 1a, b). From November 7–11, an unexpected cold surge battered East Asia. Blizzard shattered Shenyang city with 12–16 inches of snow on November 7–8, the heaviest snowstorm since 1905 (Fig. 1c). The lasting cold surge had its second wave on the 10–11, causing record-breaking early snow in Seoul and the coldest day in Miaoli, Taiwan, in the past 40 years. Following the East Asia cold air outbreak, severe flooding hit Canada and the Pacific Northwest from November 13–15 (Fig. 1d) before the ink was even dry on the climate agreements reached at the 26th UN Climate Change Conference of the Parties (COP26, October 31–November 13, 2021). The extreme storm has triggered record-shattering rainfall and severe flooding in several cities in British Columbia, which had more than 11 inches of rain, breaking a 100-year record, according to Environment and Climate Change Canada. It is among the most expensive flooding in history, with an estimated $7.5 billion loss. The floods battered much of western Washington, inundating roads and homes in the area.

The sequential clustering of extreme precipitation events from India via East Asia to North America appears to be a new form of compound disastrous weather events. It is important to investigate whether these extreme events link to each other. If they are, how are they organized? What are the conducive environmental conditions favorable for their occurrence? And what are their root causes? Addressing these questions may deepen our understanding of the origins of increasing collisions of extremes worldwide within a short time, especially as the global climate warms.

RESULTS

Asian/North American teleconnection linking the sequential precipitation extremes

The clustered precipitation extremes involve three stages. The first stage, the *Indian extreme stage*, started during the first pentad of November (1–5). It features a 'wet India-dry Philippines' precipitation pattern (Fig. 2a). Heavy precipitation occurred over southern India, the adjacent Arabian Sea, and the Bay of the Bengal (Figs. 1a and 2a). Meanwhile, suppressed convection occurs in the vicinity of the Philippines. An anomalous South Asian High emerged with a center over the Indo-China peninsula. Indian and Indonesian convective heating can generate the upper-level South Asian High[1]. The wave activity flux vectors indicate that the wave energy propagated from central Eurasia to Tibetan Plateau could favor its northwest movement and development. The wave energy propagates northeastward from the South Asian High to strengthen the upper-level East Asia Low, suggesting that anomalous Indian heating may contribute to deepening the upper-level East Asian trough and intensifying the East Asia winter monsoon. At low levels, the suppressed Philippine convection shaped an anticyclonic circulation, strengthening southwesterly from the head of the Bay of Bengal to southern China and the vertically integrated water vapor transport (IVT) (Fig. 2a right panel). An atmospheric river forms on the main seasonal path in the region[2], transporting abundant water vapor from South Asia to East Asia, preconditioning the subsequent extreme precipitation event over eastern China.

The East Asian extreme stage occurs primarily in the second pentad of November (6–10th day). The Indian rainfall anomaly moved slightly eastward and intensified (Fig. 2b), causing torrential rain in Sri Lanka (Fig. 1b). The wave energy propagated

[1]College of Atmospheric Sciences, Nanjing University of Information Science and Technology, Nanjing, China. [2]Department of Atmospheric Sciences and International Pacific Research Center, University of Hawaii, Honolulu, USA. [3]Central Weather Bureau, Taipei, Taiwan. [4]Department of Civil & Environmental Engineering, Hong Kong University of Science and Technology, Hong Kong, China. ✉email: mengqian.lu@ust.hk
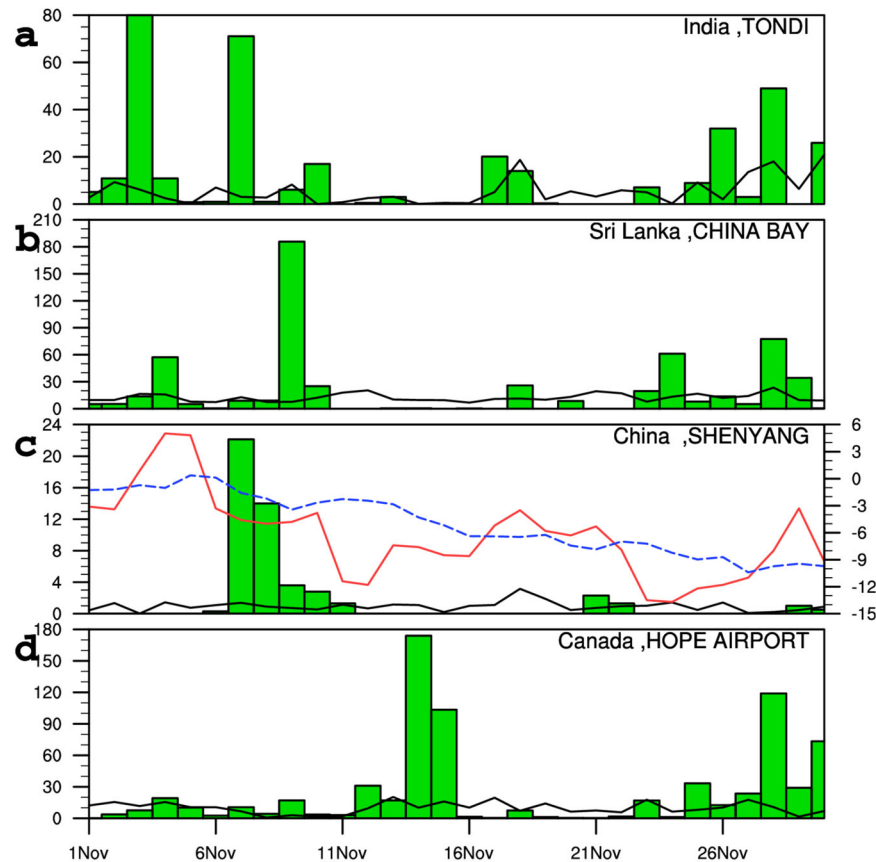
Fig. 1 Sequential extreme precipitation events from India to Canada during COP26 2021. Histograms show daily precipitation (mm) at **a** Tondi, Southern India (9.7°N, 79.0°E), **b** China Bay, Sri Lanka (8.5°N, 81.2°E), **c** Shenyang, northeast China (41.7°N, 123.5°E), and **d** Hope airport British Columbia, Canada (49.4°N, 121.5°W). The black curves denote climatology. The red curve in **c** represents the daily minimum temperature (°C), and the blue dashed curve is the corresponding climatology.

from central Eurasia to Tibetan Plateau enhances the South Asian high. Correspondingly, the South Asia High and East Asia Low were strengthened. East Asia experienced extreme early and severe cold surges, with blizzards battering northeast China (Fig. 1c). A circum-Pacific wave train was established in this stage, consisting of the South Asia High, East Asia Low, Okhotsk High, and Gulf of Alaska Low. The Rossby wave energy propagated along the great circle route[1] and invigorated the developing circum-Pacific wave train. At low levels, the cross-Pacific atmospheric rivers that emerged during the first stage persisted over this second stage, continuously making landfall on the west coast of North America.

The third stage, the North America extreme stage, is characterized by severe flooding in North America. At this stage, the South Asia rainfall anomaly extends to Southeast Asia, and the upper-level South Asia High expanded accordingly (Fig. 2c). The circum-Pacific (rim) wave train persisted and tightened. Another new cross-Pacific subtropical Rossby wave train developed. In theory[3], for a low-latitude source, long wavelengths propagate strongly poleward and eastward. Shorter wavelengths are trapped equatorward of the poleward flank of the jet, resulting in a split of the wave trains at this latitude. The action centers of this subtropical wave train tend to align with the circum-Pacific wave train in the north-south direction so that the cyclonic anomaly over the Gulf of Alaska shifted southwestward into the central North Pacific (Fig. 2c). As such, an intensive atmospheric river, called "pineapple express"[4], was established from Hawaii to the west coast of Washington state and British Columbia, transporting warm-moisture-laden air continuously to feed the devastating rainstorms over Canada and northwest U. S. during November

14–15. In fact, the cross-Pacific atmospheric rivers have been active since the beginning of November (Fig. 2a), making the west coast of North America prone to flooding with saturated soil. The landfall of "pineapple express" thus directly translated to flooding. The persistent landfalling atmospheric rivers are steered through the frontal zones within the barotropic cross-Pacific wave trains.

Mechanisms driving the Asian/North American teleconnection

The circulation pattern organizing the extreme precipitation events is named as Asian/North American (ANA) teleconnection. We hypothesize that the "wet India-dry Philippines" dipolar heating anomaly may orchestrate the subsequent circum-Pacific wave trains. While the mechanisms by which tropical convective anomalies excite stationary barotropic Rossby waves have been well established[1,5], it remains an open question how the cross-Pacific wave trains from India to North America were generated.

To this end, we have conducted a suite of numerical experiments with a linearized atmospheric general circulation model (see "Methods"). Climatological mean flows in November are specified as the basic flows. The atmospheric heat source/sink in the control experiment is represented by an idealized dipolar pattern consisting of a heating region centered in southern India and a cooling region centered in the Philippine Sea (Supplementary Fig. 1), mimicking the 'wet India-dry Philippines' dipolar heating pattern in early November (Fig. 2a).

The control experiment demonstrates that the Indian heating and Philippine cooling can excite a teleconnection pattern that resembles the observed circum-Pacific wave train, although the North Pacific anomalies are slightly weak (Fig. 3a). Wave activity
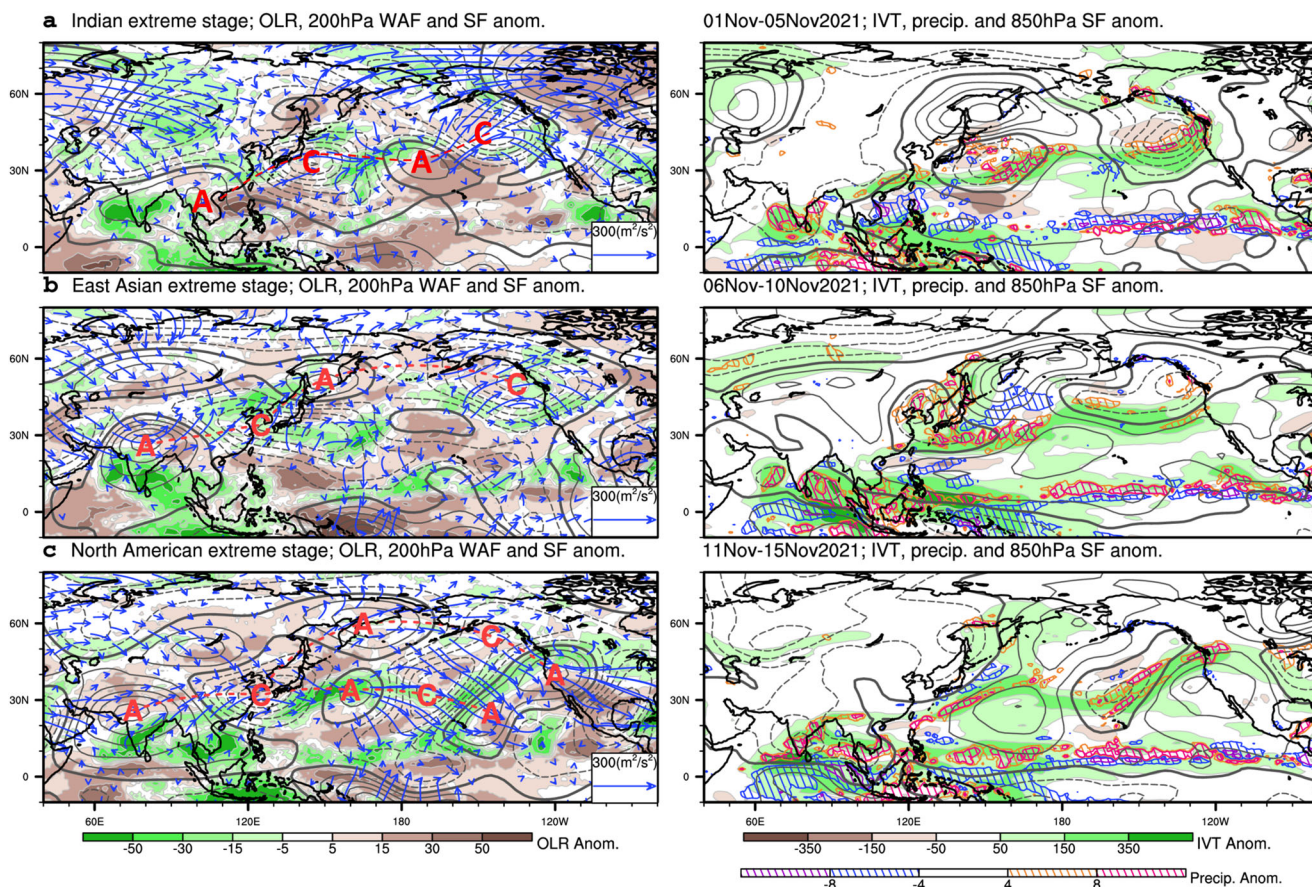
Fig. 2 Intraseasonal evolution of the atmospheric anomalies shown by pentad mean anomalies. During **a** Indian extreme stage, **b** East Asian extreme stage, and **c** North American extreme stage, left panels show OLR anomalies (shading), 200 hPa stream function anomalies (contours at an interval of $5 \times 106 \, m^2S^{-1}$), and wave activity flux (vectors) indicating energy propagation. The wave trains are highlighted by the series of A (anticyclone) and C (cyclone). Right panels exhibit atmospheric rivers by the vertically integrated water vapor transport (IVT) anomalies (shading; kg /(m*s)), with precipitation anomalies (slash filled; mm/day) and 850 hPa stream function anomalies (contour; $2.5 \times 10^6 \, m^2S^{-1}$).

flux diagnosis indicates that the wave energy generated by the Indian heating and Philippine cooling support the anomalous South Asia High and East Asia Low, respectively. The wave energy further propagates northeastward from East Asia Low to enhance the Okhotsk High and Gulf of Alaska Low. This off-equatorial diabatic heating pattern generates the Rossby wave train more effectively than equatorial heating. For comparison, we specified a heat source over the equatorial Maritime Continent centered at (10°S, 110°E). The equatorial heating produces a teleconnection pattern that mainly affects the southern hemisphere with a minor impact on the northern hemisphere (Supplementary Fig. 2).

The cross-Pacific wave trains feature two paths: one has a circum-Pacific rim route; the other mainly propagates eastward along the subtropical jet stream. In the first pentad of November, Philippine cooling dominates in the heating dipole (Fig. 2a); we mainly see the circum-Pacific wave train in the ensuing pentad (Fig. 2b). With waning Philippine cooling and strengthening Indian heating at the 2nd stage (Fig. 2b), an eastward-propagating subtropical wave train developed during the 3rd stage (Fig. 2c). This motivated us to quantify the relative roles of Indian heating and Philippine cooling in generating the two cross-Pacific wave trains. Two sensitivity experiments were conducted with a single heat source as forcing. The Indian heating forcing alone causes a low-level cyclone and an upper-level anticyclone over South Asia. The wave energy propagation is mainly from South Asia High to East Asia Low, followed by a weak eastward propagation toward the central North Pacific along the jet stream (Fig. 3b). On the other hand, Philippine

cooling stimulates a significantly stronger circulation response. It first generates a strong upper-level East Asia Low and a low-level Philippine Sea high anomaly. The wave energy then propagates primarily northeastward to enhance the Okhotsk High and Gulf of Alaska Low, forming the circum-Pacific wave train (Fig. 3c).

In sum, the off-equatorial 'wet India-dry Philippines' dipolar heating plays an essential role in generating the ANA. The Philippine cooling contributes to the circum-Pacific wave train in the midlatitude similar to the one shown in Fig. 2b during the East Asian extreme stage. On the other hand, the Indian heating enhances the eastward subtropical wave train, a pattern resembling the one shown in Fig. 2c during the North American extreme stage when the Philippine dry anomaly decays.

Although we emphasized the tropical driver of the ANA teleconnection, the midlatitude influence cannot be ruled out. The wave energy propagation from central Asia contributes to the intensification and northwest shift of the anomalous South Asian High (Fig. 2a, b). We also noticed an anomalous blocking high over Ural Mountain and a pressure trough over western Siberia and East Asia before the East Asia cold surge (Supplementary Fig. 3a). The intensified Ural Mountain High and deepening East Asian trough are conducive to East Asia cold surges[6,7]. The wave activity flux vectors shown in Supplementary Fig. 3b entail wave energy propagation from the North Atlantic to Siberia and India. The wave energy source originates from the strengthened Iceland High associated with a positive phase of North Atlantic Oscillation (NAO), suggesting a potential role of NAO in the East Asia cold surges.
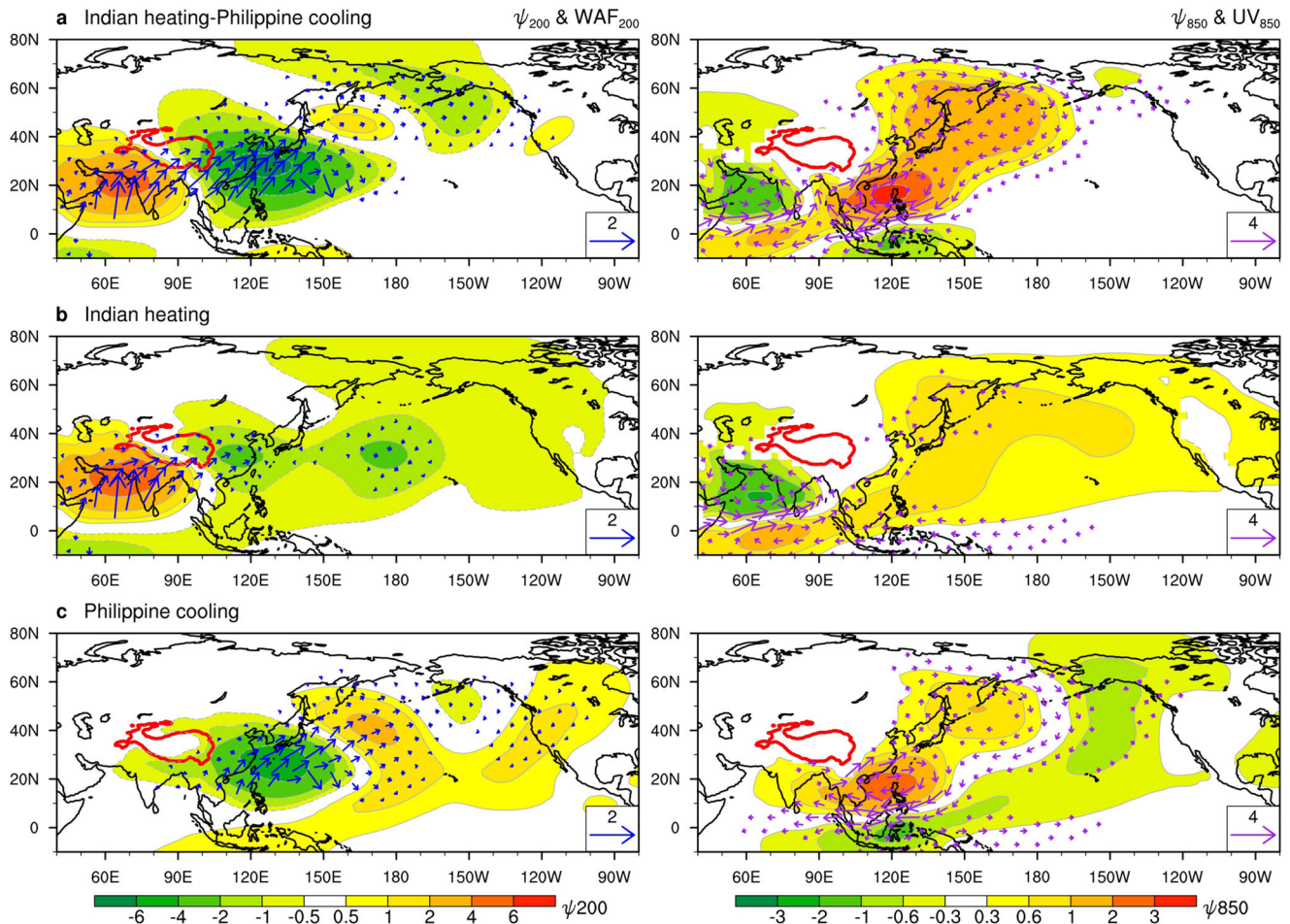
Fig. 3 Atmospheric response to the specified diabatic heating anomalies. a Dipole heating mimicking "wet India - dry Philippine", **b** Indian diabatic heating only, and **c** Philippine diabatic cooling only. Left panels show 200 hPa stream function (shading, units: $10^6\,m^2\,s^{-1}$) and wave activity flux (WAF; vector, units: $m^2\,s^{-2}$). Right panels display 850 hPa stream function (shading, units: $10^6\,m^2\,s^{-1}$) and winds (vector, units: m s^{-1}). The specified heating patterns and vertical structures are shown in Supplementary Fig. 1. The maximum (minimum) heating rate is 2 K day^{-1} (-2 K day^{-1}). The damping time scale is 5 days. The response is on Day 10. The basic state is November mean flows.

Rapidly developed La Niña sets up the "wet India-dry Philippines" condition

To identify the background conditions conducive to the 'wet India-dry Philippines' anomalous heat sources, we first examine anomalies averaged from October 15 to November 30, 2021. The 45-day mean anomalies against climatology reflect primarily interannual variations. In October, the El Niño-Southern Oscillation (ENSO) index (Niño 3.4 SST anomaly) plunged from -0.2 to $-1.0\,°C$ (Supplementary Fig. 4). By November 2021, a La Niña condition had firmly established. The SST anomalies below $-1.0\,°C$ covered the entire central and eastern Pacific (Fig. 4a).

The equatorial SST gradients generate easterly anomalies, suppressing the equatorial western Pacific convection and enhancing the Maritime Continent convection (Fig. 4b). The enhanced Maritime Continent diabatic heating can excite a pair of equatorially symmetric low-level Rossby wave-induced low pressures (hereafter Rossby wave lows)[8,9]. This type of Rossby wave response is seen over the Indian Ocean: Paired cyclones straddle the equator with prevailing equatorial westerly anomaly (Fig. 4b). The Rossby wave low (cyclonic circulation) in the Asian monsoon region extends from Malaysia to the Arabian Sea (Fig. 4b). This cyclonic circulation, in turn, can reinforce in situ precipitation via boundary layer moisture convergence, forming an anomalous South Asian rain belt. Likewise, the suppressed equatorial western Pacific diabatic heating and associated

equatorial easterly anomalies stimulate a pair of anticyclones residing on each side of the equatorial western Pacific. This Rossby wave response enhanced the western North Pacific subtropical high and reduced precipitation near the Philippines.

In summary, the 2021 La Niña installs an anomalous low-level quadrupole circulation pattern with a pair of cyclones straddling the Indian Ocean and double anticyclones over the western Pacific (Fig. 4b). The La Niña sets up a 'wet India-dry Philippines' anomaly pattern in the Asian-western North Pacific monsoon regions.

Quasi-stationary MJO bolsters the "wet India-dry Philippines" dipole pattern

The ANA teleconnection occurs on a global scale and beyond the weather time scale. Hence, we further zoom in on the evolution of the pentad mean anomalies that depict the intraseasonal atmospheric variability. With the La Niña background, an MJO[10] event developed over the Indian Ocean in early November. Consistent with the slow-moving convective anomalies (Fig. 5a–c), the Real-time Multivariate MJO index[11] widely used for monitoring the MJO circulation system affirms that the MJO stalled over the western Maritime Continent from November 4 to 20 (Fig. 5d). The low-level westward propagating Rossby wave lows and associated convective anomalies emanated from the western Maritime Continent, form an anomalous zonal rain belt over South Asia (Fig. 5a–c). Meanwhile, the MJO convective heating at the western Maritime Continent
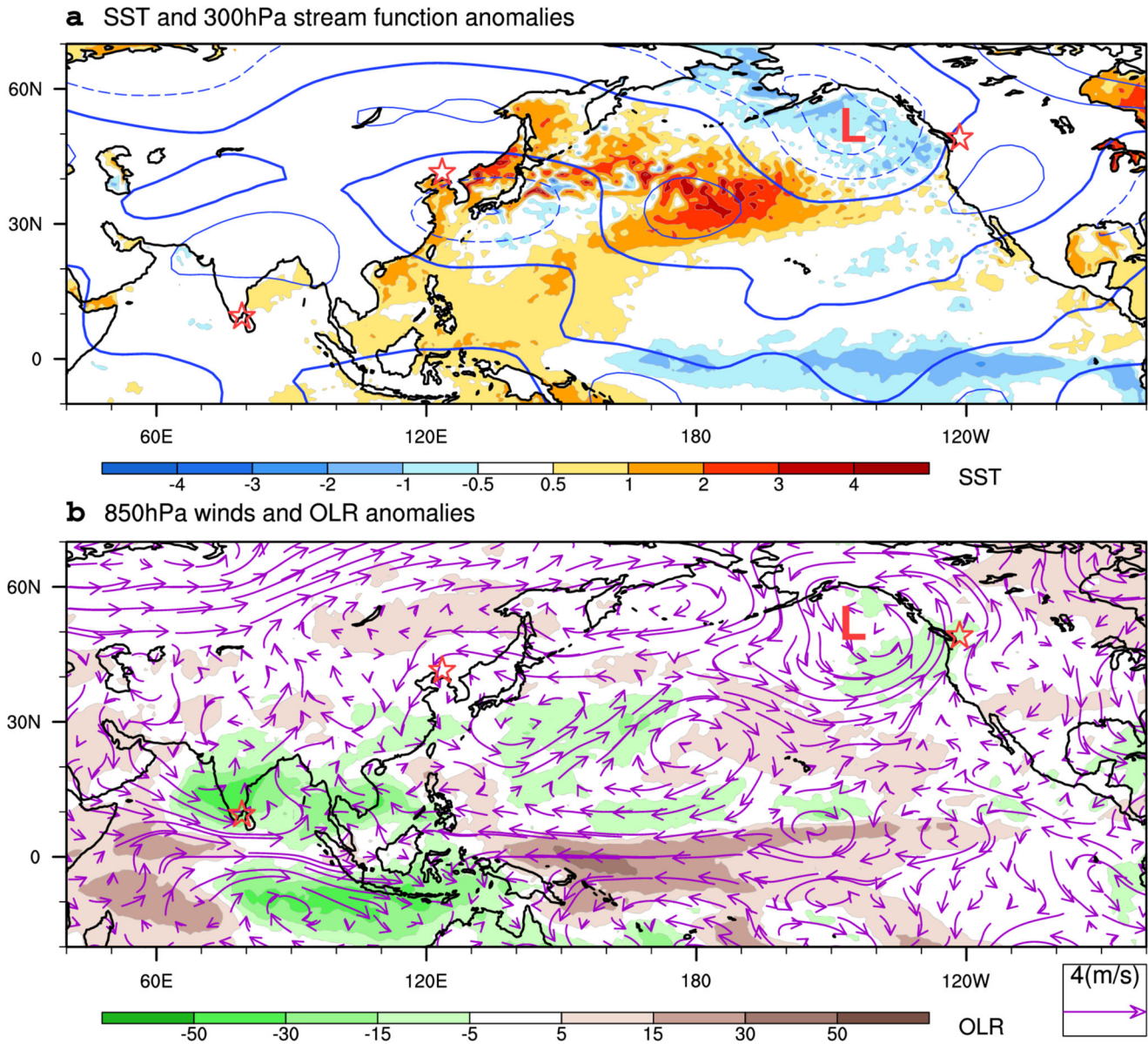
a SST and 300hPa stream function anomalies

b 850hPa winds and OLR anomalies

Fig. 4 Climate mean anomalies averaged from October 15 to November 30, 2021. a SST (shading) and upper-level (300 hPa) stream function (contours with interval at 5×10^6 m^{2}S^{-1}) anomalies. **b** Low-level (850 hPa) winds and outgoing longwave radiation (OLR) anomalies (shading). The stars indicate locations of extreme weather events over India, northeast China, and Canada. The Gulf of Alaska Low is marked.

generates intense easterlies over the western Pacific as a Kelvin wave response. The easterlies-induced meridional shear vorticity strengthens the anticyclone in the Philippine Sea, suppressing convection and sustaining an anomalous cooling center.

Note that the MJO-induced convective anomalies are significantly more intense than the La Niña-induced counterparts, especially over the Philippines (Figs. 4b and 5a, b). Thus, the MJO convective anomalies strongly reinforce the "wet India-dry Philippines" dipole precipitation pattern that La Niña sets up. This stationary pattern provides continuing condensational heat/cooling sources to fortify the ANA teleconnection circulation anomalies during the three-stage evolution of the clustered extreme events.

DISCUSSION

Figure 6 summarizes our key findings. The COP26 clustered extreme precipitation events, including the severe India-Sri Lanka flooding, the East Asian blizzard, and the Canadian floods, are organized by an intraseasonal Asian/North American (ANA) teleconnection consisting of the South Asia High, East Asia Low, Okhotsk High, Gulf of Alaska Low, and California High (Fig. 6a).

Our numerical experiments suggest that the "wet India-dry Philippines" dipolar diabatic heating fortifies ANA teleconnection by generating two cross-Pacific wave trains (Fig. 6c). Indian heating induces a subtropical cross-Pacific wave train along the jet stream. In contrast, the Philippine heat source stimulates a midlatitude circum-Pacific wave train under November mean state. The dipole heating anomaly is set up by the quadrupolar circulation anomalies induced by the rapidly developed La Niña and further bolstered by the quasi-stationary MJO, preferably occurring during La Niña (Fig. 6b, c). The combined effects of the dipolar heating during late Fall are demonstrated for the first time. It would be interesting to explore how the atmosphere responds to such dipole heating during boreal summer or other seasons.

The ANA teleconnection is a new route by which ENSO and MJO may affect North America. It differs from Pacific/North American
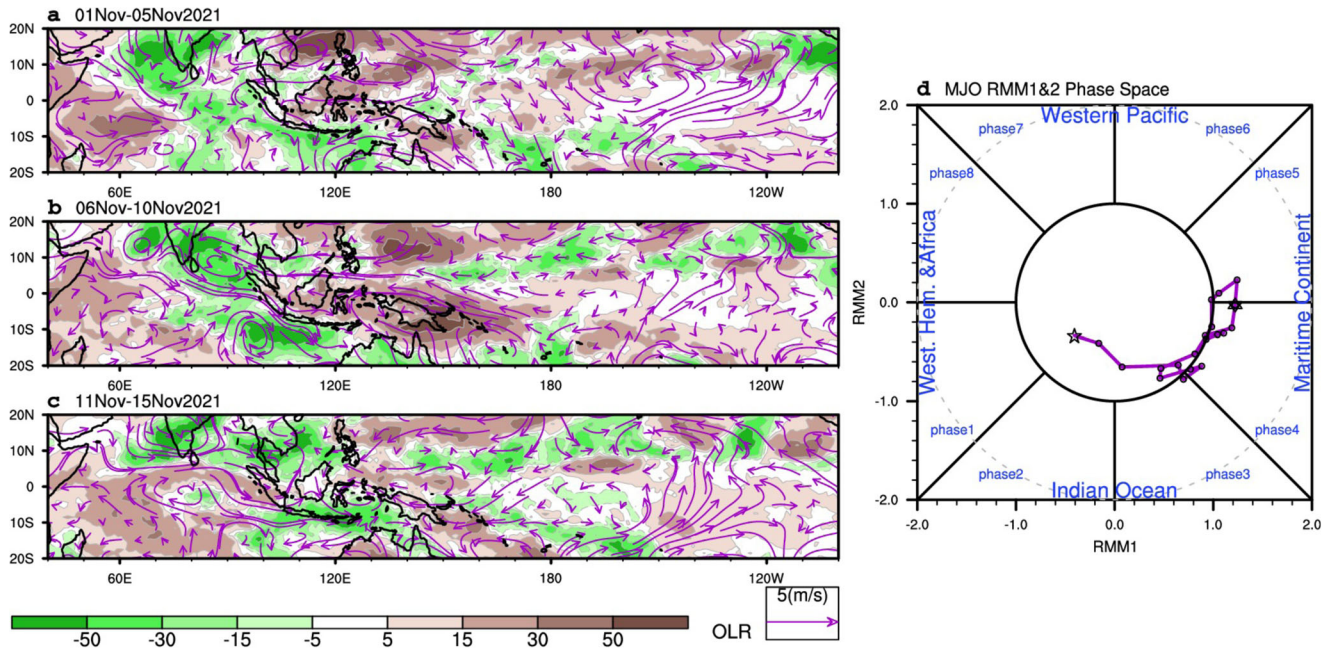
Fig. 5 Quasi-stationary Madden-Julian Oscillation (MJO) in November 2021. Pentad mean of filtered OLR (see 'Data') and 850 hPa winds anomalies associated with the MJO during (**a**) November 1–5, **b** November 6–10, and **c** November 11–15, 2021. **d** Real-time Multivariate MJO (RMM) indices shown in the phase plane expanded by RMM1 and RMM2 from November 1 to November 20, 2021. MJO stays in the western Maritime Continent (Phase 4) from November 1 to 20, 2021.

(PNA) teleconnection[12], which is strongly influenced by ENSO-induced central Pacific precipitation anomalies. PNA features the anomalous Gulf of Alaska and Aleutian Low (High) during El Niño (La Niña)[13,14]. Thus, the Gulf of Alaska Low in ANA eminent during the 2021 La Niña is not a PNA response to the central Pacific heating associated with ENSO. Instead, the ANA teleconnection is coerced by the "wet India-dry Philippines" dipolar heating resulting from the multi-scale interaction between the rapidly developing La Niña and the quasi-stationary MJO.

The fundamental cause of the quasi-stationary MJO event is rooted in the La Niña condition. MJO exhibits diversified propagation patterns[15]. One of them is quasi-stationary. Namely, the propagation over the Indian Ocean stopped when reaching the Maritime Continent. The stationary MJO events preferably occur when the equatorial central Pacific is abnormally cold[15]. Thus, La Niña made the MJO event stagnate over the Maritime Continent. On the other hand, the quasi-stationary MJO event, in turn, reinforced the 'wet India-dry Philippines' initiated by La Niña. The result suggests multi-scale interactive feedback between the La Niña and quasi-stationary MJO over the tropical Asian monsoon region, giving rise to intense and continuous convective heating anomalies, sustaining ANA and a chain of extreme weather events from tropics to high latitudes.

MJO affecting extratropics through an off-equatorial "wet India-dry Philippines" dipolar heating is a new phenomenon that differs from the existing MJO teleconnections. The previous MJO teleconnection studies focus on the equatorial convective anomalies produced by MJO, not the off-equatorial heat sources[16–19]. When MJO convection is located in the equatorial Indian Ocean (IO), the western Pacific (WP) features a dry anomaly during MJO phases 2 and 3. This equatorial IO-WP dipolar heating tends to generate a consistent PNA-like MJO teleconnection pattern due to the constructive interference of similar teleconnection signals induced by the IO and WP heat sources[19]. ENSO can significantly modify this teleconnection pattern[18]. However, the off-equatorial "wet India-dry Philippines" dipolar heating occurs during MJO phase 4 when MJO convection is located in the western Maritime Continent. It is induced by the combined effects of La Niña and MJO. The off-equatorial dipolar

heating produces two cross-Pacific Rossby wave trains that differ from the MJO teleconnection. The off-equatorial dipolar heating is more effective in stimulating circum-global teleconnection with a boreal summer mean state[20,21]. It remains unknown how often MJO produces such an off-equatorial dipole heating during late Fall and does so through what specific processes.

The Atmospheric River has been chiefly analyzed on an hourly-to-daily scale for contemporaneous associations with severe weather events. Here we documented cross-Pacific atmospheric rivers embedded in the intraseasonal wave trains causing clustering extreme precipitation events. It might be interesting to see how often we see similar low-frequency atmospheric rivers and assess their roles in sequential extreme precipitation events.

Our study provides a new perspective on future precipitation variability by emphasizing the clustering of extreme precipitation events with escalated compound impact beyond their simple addition. The occurrence of the early November snowstorms over East Asia implies that although global warming may delay the start of the winter in general[22], extreme snowstorms and cold surges may occur earlier in late Fall, causing unexpected damage. Besides, the sequential clustering of extreme events might offer a predictability source because their favorable atmospheric precursors stem from the tropics associated with the rapid La Niña cooling. It poses the question of whether there are ongoing changes in the routes of how tropics and extratropics interact. Our results imply that the multi-scale and tropical-extratropical interaction under a warming world may cause more frequent compound disasters worldwide due to increasing water vapor availability. However, more in-depth case analyses and modeling simulations are required to deepen our understanding of the potential future change in the states of extreme precipitation occurrence.

METHODS

Data
We used daily station precipitation data in November 2021 from the Global Historical Climatology Network to depict the clustering
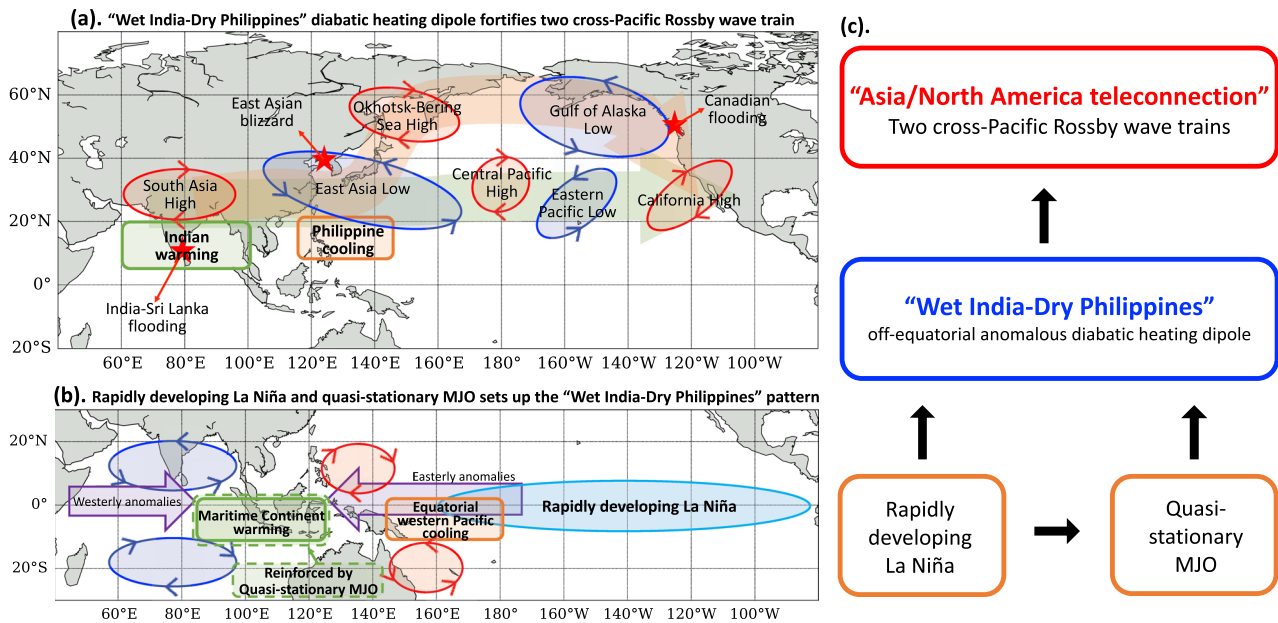
Fig. 6 Summary schematics. a the Asian/North American teleconnection organizing the cluster of sequential extreme precipitation events, **b** the "wet India-dry Philippine" diabatic heating generated by rapidly developed La Nina and quasi-stationary MJO, and **c** the causality mechanism.

of extreme events over the four areas in Fig. 1. The Niño 3.4 is provided by NOAA Climate Prediction Center. Other variables, including precipitation, horizontal winds at 200/300/850 hPa, and vertically integrated water vapor transport, are retrieved from NCEP–NCAR Reanalysis 1[23], NOAA Optimum Interpolation Sea Surface Temperature (OISST) V2[24] and ERA5 reanalysis[25]. The daily OLR values are from the Daily Climate Data Record. The anomalous fields were obtained by removing the climatological seasonal cycle. To depict the deep convection and circulation associated with the MJO, we use filtered OLR and circulation anomalies in Fig. 5 by removing the seasonal cycle (the mean and first three harmonics of the climatological annual variation) as well as the interannual variability by subtracting the running mean of the previous 120 days as constructing the Real-time Multivariate MJO index[4].

Atmospheric models used and numerical experiment design

A dry version of a linearized AGCM, Linear Baroclinic Model (LBM)[26], is used for numerical experiments. This model has a horizontal resolution of T42 and 20 vertical sigma levels. We neglected moist convection to focus on dynamic processes. The damping time scale is set at 1 day for the lowest three levels and the topmost two levels and set at 5 days elsewhere. The basic state is set as the climatological November mean flow.

We performed four experiments by imposing different convective heating forcing respectively: (a) Indian heating-Philippine cooling dipole, (b) Indian heating only, (c) Philippine cooling only, and (d) Equatorial Maritime Continent heating. The Indian heating forcing is centered at (13°N, 80°E), and the Equatorial Maritime Continent heating forcing is centered at (10°S, 110°E). They have a maximum heating rate of $2\,\mathrm{K\,day^{-1}}$ at the 0.45 sigma level. Similarly, The Philippines cooling forcing is centered at (15°N, 130°E) with a minimum heating rate of $-2\,\mathrm{K\,day^{-1}}$ at the 0.45 sigma level.

DATA AVAILABILITY
All data have been deposited on Zenodo with DOI: 10.5281/zenodo.7243472.

CODE AVAILABILITY
The scripts to construct the figures and perform the numerical experiments have been deposited on Zenodo with DOI: 10.5281/zenodo.7243472.

REFERENCES
1. Hoskins, B. J. & Karoly, D. J. Steady linear response of a spherical atmosphere to thermal and orographic forcing. *J. Atmos. Sci.* **38**, 1179–1196 (1981).
2. Pan, M. & Lu, M. East Asia Atmospheric River catalog: annual cycle, transition mechanism, and precipitation. *Geophys. Res. Lett.* **47**, e2020GL089477 (2020).
3. Ambrizzi, T., Hoskins, B. J. & Hsu, H. H. Rossby wave propagation and teleconnection patterns in the austral winter. *J. Atmos. Sci.* **52**, 3661–3672 (1995).
4. Gimeno, L., Nieto, R., Vázquez, M. & Lavers, D. A. Atmospheric rivers: a mini-review. *Front. Earth Sci.* **2**, 2 (2014).
5. Sardeshmukh, P. D. & Hoskins, B. J. Generation of global rotational flow by steady idealized tropical divergence. *J. Atmos. Sci.* **45**, 1228–1251 (1988).
6. Ding, Y., Wang, Z., Song, Y. & Zhang, J. Causes of the unprecedented freezing disaster in January 2008 and its possible association with the global warming. *Acta Meteorol. Sin.* **66**, 808–825 (2008).
7. Dong, S., Ding, Y. & Jiang, D. A low-frequency downstream development process leading to the outbreak of a mega-cold wave event in East Asia. *J. Meteorol. Soc. Jpn.* **99**, 1185–1200 (2021).
8. Matsuno, T. Quasi-geostrophic motions in the equatorial area. *J. Meteorol. Soc. Jpn.* **44**, 25–43 (1966).
9. Gill, A. E. Some simple solutions for heat-induced tropical circulation. *Q. J. R. Meteorol. Soc.* **106**, 447–462 (1980).
10. Madden, R. A. & Julian, P. R. Description of global-scale circulation cells in the tropics with a 40-50 day period. *J. Atmos. Sci.* **29**, 1109–1123 (1972).
11. Wheeler, M. C. & Hendon, H. H. An All-Season Real-Time Multivariate MJO Index: development of an index for monitoring and prediction. *Monthly Weather Rev.* **132**, 1917–1932 (2004).
12. Wallace, J. M. & Gutzler, D. S. Teleconnections in the geopotential height field during the Northern Hemisphere winter. *Monthly Weather Rev.* **109**, 784–812 (1981).
13. Bjerknes, J. Atmospheric teleconnection from the equatorial Pacific. *Monthly Weather Rev.* **97**, 163–172 (1969).
14. Lau, N. C. & Nath, M. J. The role of the "atmospheric bridge" in linking tropical Pacific ENSO events to extratropical SST anomalies. *J. Clim.* **9**, 2036–2057 (1996).
15. Wang, B., Chen, G. & Liu, F. Diversity of the Madden-Julian Oscillation. *Sci. Adv.* **5**, eaax0220 (2019).

16. Lau, K. M. & Philips, T. J. Coherent fluctuations of extratropical geopotential height and tropical convection in intraseasonal time scales. *J. Atmos. Sci.* **43**, 1164–1181 (1986).
17. Higgins, R. W. & Mo, K. C. Persistent north Pacific circulation anomalies and the tropical intraseasonal oscillation. *J. Clim.* **10**, 223–244 (1997).
18. Moon, J. Y., Wang, B. & Ha, K. J. ENSO regulation of MJO teleconnection. *Clim. Dyn.* **37**, 1133–1149 (2011).
19. Tseng, K.-C., Maloney, E. & Barnes, E. The consistency of MJO teleconnection patterns: an explanation using linear Rossby wave theory. *J. Clim.* **32**, 531–548 (2019).
20. Ding, Q. & Wang, B. Circumglobal teleconnection in the Northern Hemisphere Summer. *J. Clim.* **18**, 3483–3505 (2005).
21. Moon, J. Y., Wang, B. & Ha, K. J. Teleconnections associated with Northern Hemisphere summer monsoon intraseasonal oscillation. *Clim. Dyn.* **40**, 2761–2774 (2013).
22. Wang, B. et al. Monsoons climate change assessment. *Bull. Am. Meteorol. Soc.* **102**, E1–E19 (2021).
23. Kalnay, E. et al. The NCEP/NCAR 40-year reanalysis project. *Bull. Am. Meteorol. Soc.* **77**, 437–470 (1996).
24. Reynolds, R. W., Rayner, N. A., Smith, T. M., Stokes, D. C. & Wang, W. An improved in situ and satellite SST analysis for climate. *J. Clim.* **15**, 1609–1625 (2002).
25. Hersbach, H. et al. Global reanalysis: goodbye ERA-Interim, hello ERA5. *ECMWF Newsl.* **159**, 17–24 (2019).
26. Watanabe, M. & Kimoto, M. Atmosphere-ocean thermal coupling in the North Atlantic: a positive feedback. *Q. J. R. Meteorol. Soc.* **126**, 3343–3369 (2000).

AUTHOR CONTRIBUTIONS

B.W. and M.L. conceptualized the study. M.L. contributed to data collection and analysis. Z.X. performed model experiments. M.P. contributed to the atmospheric river analysis. B.W. interpreted the results. B.W. and M.L. wrote the drafts. All contributes to review and improve the manuscript.

COMPETING INTERESTS

The authors declare no competing interests.

ADDITIONAL INFORMATION

Supplementary information The online version contains supplementary material available at https://doi.org/10.1038/s41612-022-00318-7.

Correspondence and requests for materials should be addressed to Mengqian Lu.

Reprints and permission information is available at http://www.nature.com/reprints

Publisher's note Springer Nature remains neutral with regard to jurisdictional claims in published maps and institutional affiliations.